A novel cathode material BaCe0.4Sm0.2Co0.4O3−δ for proton conducting solid oxide fuel cell

2 AUTHORS:

Cuijuan Zhang
The University of Calgary
18 PUBLICATIONS **236** CITATIONS

SEE PROFILE

Hailei Zhao
University of Science and Technology Beijing
169 PUBLICATIONS **2,013** CITATIONS

SEE PROFILE

A novel cathode material $BaCe_{0.4}Sm_{0.2}Co_{0.4}O_{3-\delta}$ for proton conducting solid oxide fuel cell

Cuijuan Zhang [a], Hailei Zhao [a,b,*]

[a] School of Materials Science and Engineering, University of Science and Technology Beijing, Beijing 100083, China
[b] Beijing Key Lab of New Energy Material and Technology, Beijing 100083, China

ARTICLE INFO

ABSTRACT

A novel cathode material $BaCe_{0.4}Sm_{0.2}Co_{0.4}O_{3-\delta}$ composed of two phases $BaCe_{1-x}(Sm/Co)_xO_{3-\delta}$ and $BaCo_{1-x}(Sm/Ce)_xO_{3-\delta}$ was prepared *in situ* via the citric–nitrate route and its performance as cathode material for proton conducting solid oxide fuel cell (SOFC-H) was characterized. $BaCe_{0.4}Sm_{0.2}Co_{0.4}O_{3-\delta}$ exhibited simultaneous protonic, electronic, and oxygen ionic conduction in air, leading to a good electrode performance. The polarization resistance of the novel cathode material in symmetrical cell was 0.36 Ω cm^2 with Pt as the current collector at 700 °C in wet air. The electrode performance can be further improved through microstructure optimization. It also showed good thermal expansion compatibility with $BaCe_{0.8}Sm_{0.2}O_{3-\delta}$ electrolyte over a 100 h duration test. $BaCe_{0.4}Sm_{0.2}Co_{0.4}O_{3-\delta}$ is a promising cathode material for SOFC-H.

© 2011 Elsevier B.V. All rights reserved.

1. Introduction

Proton conducting solid oxide fuel cell (SOFC-H) exhibits several advantages over its oxygen ion based analogue (SOFC-O) in terms of lower operation temperature and higher efficiency [1]. However, the maximum power density of single SOFC-H cell achieved (~1100 and ~660 mW cm^{-2} at 750 and 650 °C, respectively [2]) is much lower than that of SOFC-O. One of the great challenges for the development of high performance SOFC-H lies in the discovery of appropriate cathode materials; the present cathode materials for SOFC-H are mostly transferred from SOFC-O. Besides the similar requirements for cathode materials for both kinds of SOFCs, an ideal cathode material for SOFC-H should also conduct proton to maximize the triple phase boundaries (TPBs) [3–5].

To achieve the simultaneous conduction of electron, oxygen ion and proton in air, a simple method is to prepare composite cathode by mixing oxygen ionic–electronic conductor and protonic conductor such as $La_{0.6}Sr_{0.4}Co_{0.2}Fe_{0.8}O_{3-\delta}$-$BaZr_{0.1}Ce_{0.7}Y_{0.2}O_{3-\delta}$ (LSCF-BZCY) [2], $Sm_{0.5}Sr_{0.5}CoO_{3-\delta}$-$BaCe_{0.8}Sm_{0.2}O_{3-\delta}$ (SSC-BCS) [4,5], $La_{0.6}Sr_{0.4}Co_{0.2}Fe_{0.8}O_{3-\delta}$-$BaCe_{0.9}Yb_{0.1}O_{3-\delta}$ (LSCF-BCYb) [6] and $Pr_{0.58}Sr_{0.4}Fe_{0.8}Co_{0.2}O_{3-\delta}$-$BaCe_{0.9}Yb_{0.1}O_{3-\delta}$ (PSFC-BCYb) [7]. In this case, the homogeneous distribution and proper ratio between the two components are required to achieve percolation path. Another approach is to dope the proton conductor with transition metals, e.g., $BaCe_{0.9-x}Y_{0.1}(Fe/Mn/Co)_xO_{3-\delta}$ [8], $BaCe_{0.7}Zr_{0.1}Y_{0.2-x}Co_xO_{3-\delta}$ [9], $BaCe_{0.9-x}Y_{0.1}Ru_xO_{3-\delta}$ [10]. The

doping level must be low to obtain single phase, thus the introduced electronic conductivity is limited.

Here, we developed a novel cathode material for SOFC-H. High fraction of transition metal was introduced into the proton conductor matrix to produce *in situ* a two-phase composite with homogeneous distribution. The simply synthesized $BaCe_{0.4}Sm_{0.2}Co_{0.4}O_{3-\delta}$ had a low polarization resistance and can be potential cathode material for SOFC-H.

2. Experimental

The $BaCe_{0.4}Sm_{0.2}Co_{0.4}O_{3-\delta}$ (BCSC) powder was synthesized through the citric–nitrate method [11]. The as-combusted powder was calcined at 900 °C for 10 h and then at 1100 °C for 10 h. The resultant powder was further fired at 1200, 1250, 1300 °C for 2 h to study the phase evolution. The powder fired at 1100 °C was uniaxially pressed into pellets and subsequently sintered at 1200 °C for 5 h. The densed pellets with relative density of ~95% were used for electrical conductivity measurement.

Symmetrical cells with the configuration of BCSC|$BaCe_{0.8}Sm_{0.2}O_{3-\delta}$ (BCS)|BCSC were used for the impedance studies. The dense BCS pellets (~11.5 mm in diameter and ~0.5 mm in thickness) were prepared by sintering at 1500 °C for 5 h [11]. The BCSC powder calcined at 1100 °C was mixed with 20% starch pore former by hand grinding and screen printed symmetrically on both sides of the BCS pellets, followed by calcining at 1200 °C for 2 h in air. Platinum paste was painted on the electrodes and fired at 900 °C for 0.5 h as the current collector.

The phase composition of BCSC was examined by X-ray diffraction (XRD, Rigaku D/MAX-RB) with Cu Kα radiation at room temperature.

---

* Corresponding author at: School of Materials Science and Engineering, University of Science and Technology Beijing, Beijing 100083, China. Tel./fax: +86 10 82376837.
E-mail address: hlzhao@ustb.edu.cn (H. Zhao).

Scanning electron microscope (SEM, LEO-1450) was employed to detect the electrode microstructure. The electrical conductivity of BCSC and the electrode performance of symmetrical cells were measured with a Solartron 1260 frequency response analyzer coupled with the 1287 potentiostat with a signal amplitude of 5 mV under open circuit voltage (OCV) condition in the frequency range of 0.1–10^6 and 0.01–10^6 Hz, respectively. The electrical conductivity of BCSC was measured in dry and wet ($p(H_2O/D_2O) = 0.074$ atm) air, and atmospheres of different oxygen partial pressures with the gas flowing through water at room temperature. The oxygen partial pressure was varied between 0.05 and 1 atm by mixing air or oxygen with Ar using flowmeters. The symmetrical cell test was performed in wet atmospheres ($p(H_2O) \approx 0.053$ atm).

3. Results and discussions

Fig. 1 shows the phase evolution of BCSC with temperature. The XRD pattern of BCS [11] is included. The shift of the diffraction peaks in BCSC comparing with the pure BCS and $BaCoO_3$ (ICSD #28865) indicated that some Co dissolved into the $BaCe_{0.8}Sm_{0.2}O_{3-\delta}$ lattice and Sm and/or Ce into the $BaCoO_3$ lattice. The two phases of $BaCe_{1-x}(Sm/Co)_xO_{3-\delta}$ and $BaCo_{1-x}(Sm/Ce)_xO_{3-\delta}$ can be obtained at 1200 °C although with trace of Ba_2CoO_4 impurity. The distribution of all the elements was homogeneous as revealed by SEM element mapping. Therefore, a two phase composite was produced *in situ* in BCSC. The tolerance factor (t) of BCS and $BaCoO_3$ is estimated to be 0.93 and 1.02, respectively. The shift of the peak position inferred that the t values tended to be unity for the two components in BCSC, corresponding to cubic structure, which is desirable for structural stability. Doped $BaCeO_3$ exhibits protonic and electronic conduction in air [1] while doped $BaCoO_3$ (cubic phase) is a good mixed oxygen ionic–electronic conductor [12], the BCSC material was expected to exhibit good electrical conductivity.

To investigate the electrical conduction behavior of BCSC, the electrical conductivity in different atmospheres was measured and the Arrhenius plots are presented in Fig. 2. At temperatures ≤550 °C, the electrical conductivity in wet air is slightly higher than that in dry air. Meanwhile, the conductivity in D_2O-air was lower than that in H_2O-air. Both indicated the proton conduction at low temperatures. However, the contribution of proton conduction is small because the ratio of the conductivity values in H_2O-air to that in D_2O-air was 1.01–1.03 and an increase in E_a of only 0.002 eV was observed in D_2O-air atmospheres. At elevated temperatures ≥600 °C, the electrical conductivity in dry and wet (H_2O/D_2O) air merged. Furthermore, the electrical conductivity increased with $p(O_2)$ over the whole temperature range (Fig. 2(b)). Accordingly, it is reasonable to state that the mixed oxygen ionic–electronic conduction dominated over the whole temperature range studied. Nevertheless, the small contribution of proton conduction can effectively extend the TPBs,
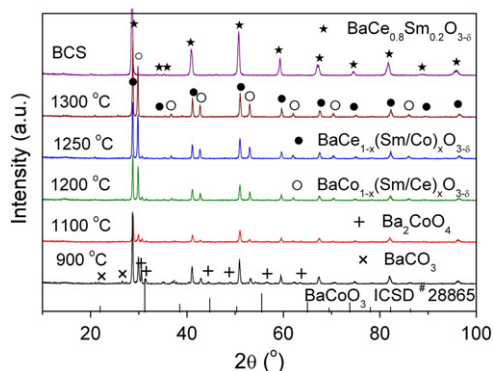
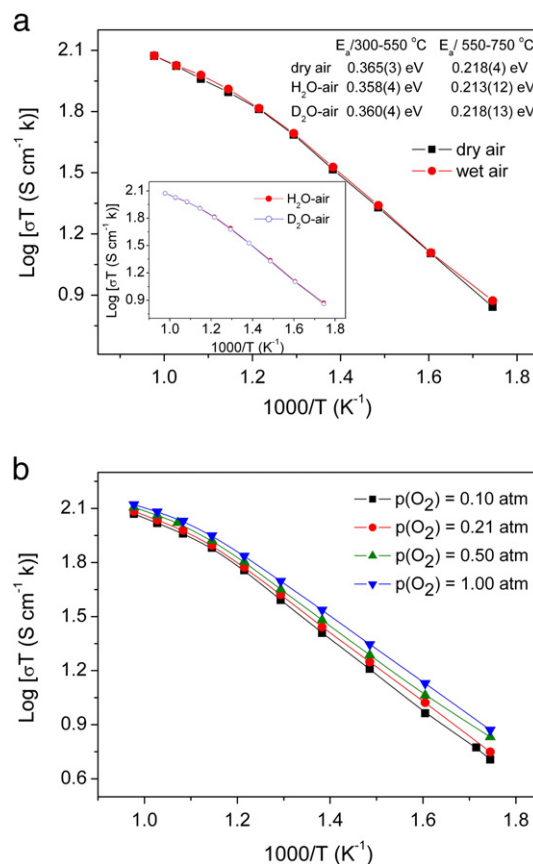**Fig. 1.** XRD patterns of BCSC calcined at different temperatures and BCS sintered at 1500 °C.

Fig. 2. Electrical conductivity of BCSC in dry and wet air (a); Electrical conductivity of BCSC as a function of $p(O_2)$ (b).

which is beneficial for the improvement of cathode performance, as discussed below.

The performance of BCSC cathode was measured on symmetrical cells of BCSC|BCS|BCSC with Pt as the current collector. The polarization resistance (R_p) of BCSC in wet air is displayed in Fig. 3 (a). The R_p of some composite cathodes in literature was also included for comparison. The performance of the BCSC cathode was comparable with that of some reported composite cathodes. R_p was 0.36 Ω cm² at 700 °C. It should be noted that the performance of composite cathodes [5–7] was tested with Ag as the current collector. Ag is an excellent catalyst for oxygen adsorption, dissociation and diffusion [13]. In fact, with Ag as the current collector, the BCSC electrode exhibited better performance (included in Fig. 3(a)) than the composite cathodes [5–7]. Considering the low porosity of the present BCSC cathode (see Fig. 4), the performance can be further enhanced through microstructure optimization.

To explore the possible reasons for the good performance of BCSC, impedance in different oxygen partial pressures ($p(O_2)$) was measured. The Nyquist plot of the symmetrical cells can be separated into three semi-circles, which were fitted with $R_{ohm}(R_1Q_1)(R_2Q_2)(R_3Q_3)$ from high to low frequencies. R and Q represent corresponding resistance and capacitance, respectively. The spectroscopy at 700 °C in air is inset in Fig. 3(a). The Arrhenius plots of fitted R_1, R_2 and R_3 are shown in Fig. 3(b)–(d), respectively. The m_i index in $R_i = Kp(O_2)^{-m_i}$ at different temperatures is inset.

The oxygen reduction on the cathode of SOFC-H is a complex process with several steps and different steps correspond to different E_a and m values [4,14]. For the processes related to R_2 and R_3, the corresponding m values (~ 0.25, 0.34–0.48) were comparable with those for the similar processes for SSC-BCS reported by He et al. [4]. It indicated that the diffusion of O^-_{ad} ($O^-_{ad} \rightarrow O^-_{TPB}$) and the electron charge transfer ($O_{ad} + e^- \rightarrow O^-_{ad}$) contributed to these processes,
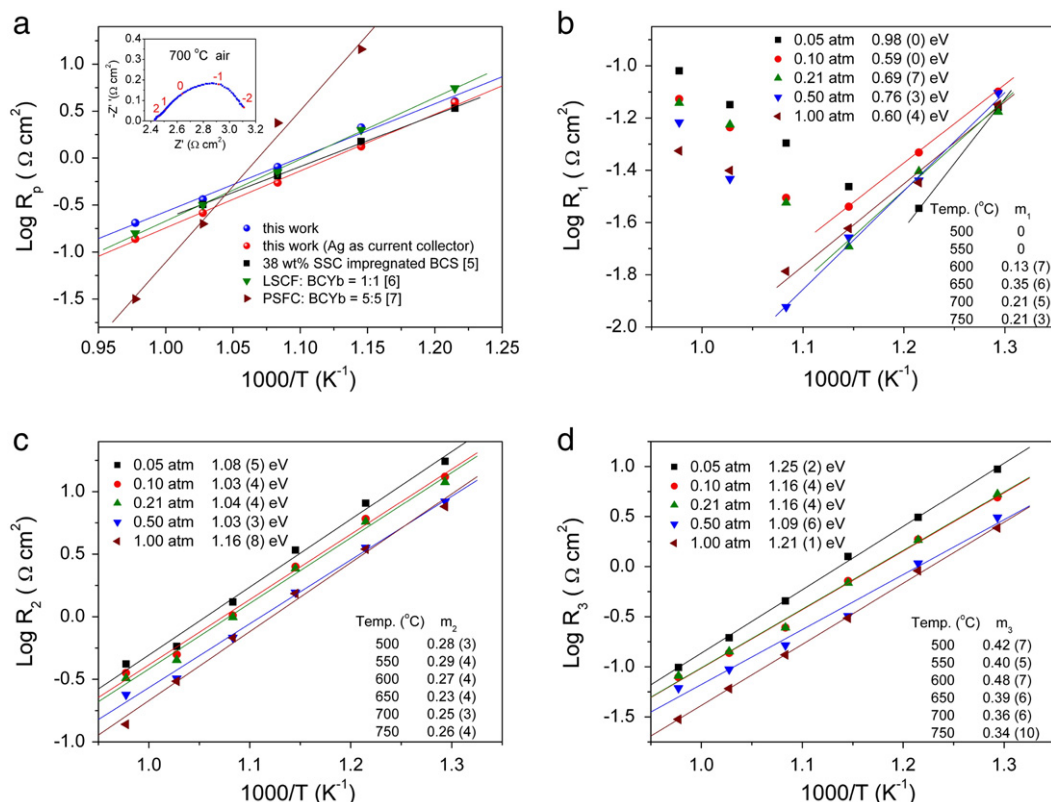
Fig. 3. Comparison of polarization resistance of the BCSC cathode in wet air with the reported composite cathodes (a). Temperature dependence of R_1 (b), R_2 (c) and R_3 (d) for BCSC cathode at different $p(O_2)$. The spectroscopy at 700 °C in wet air and the m index at different temperatures were inset.

respectively, which were also the rate-limiting steps for the BCSC cathodes on the BCS electrolyte. The process related to R_1 was probably originated from the proton diffusion in the interface between the BCSC cathode and the BCS electrolyte because the activation energy of 0.60–0.76 eV is quite close to that of proton conduction in $BaCeO_3$-based oxides [1]. Similar process has been observed in the composite cathode [4–7]. However, the magnitude of R_1 is much lower than that of the composite cathode, e.g., R_1 is 0.067 Ω cm^2 at 500 °C in air while it is 2.07 Ω cm^2 under similar condition for the SSC-BCS composite cathode [4]. Accordingly, it is reasonable to state that the proton conductivity in the BCSC cathode is high, which expands the TPBs to the whole electrode, leading to the improved electrode performance.
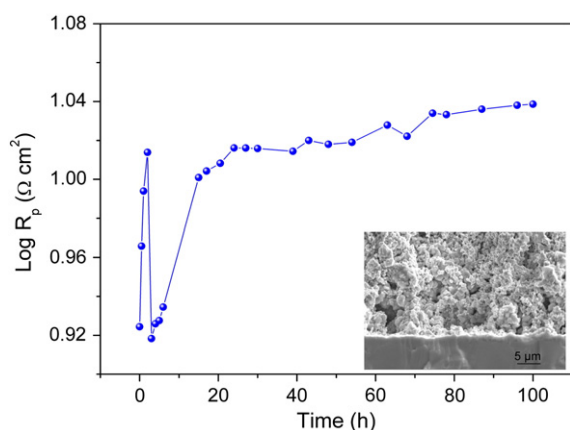

Fig. 4. Long term stability of BCSC cathode in symmetrical cell at 650 °C in wet air under OCV condition. SEM micrograph of the BCSC–BCS interface after test was inset.

To further study the long term performance of BCSC cathode on BCS electrolyte, the symmetrical cell was subjected to 100 h test at 650 °C in wet air under OCV condition. As shown in Fig. 4, R_p varied with time initially and then remained almost constant over the 100 h duration. The SEM micrograph of the BCSC cathode and BCS electrolyte interface after test is inset. The cathode and the electrolyte had a good bonding and continuous contact at the interface. No delamination or crack was observed, suggesting a good thermal expansion compatibility of the BCSC cathode with the BCS electrolyte.

4. Conclusions

A novel $BaCe_{0.4}Sm_{0.2}Co_{0.4}O_{3-\delta}$ cathode for SOFC-H was developed and its conductivity and electrode performance was investigated. The BCSC was a two-phase composite of $BaCe_{1-x}(Sm/Co)_xO_{3-\delta}$ and $BaCo_{1-x}(Sm/Ce)_xO_{3-\delta}$ synthesized *in situ* via citric–nitrate route at 1200 °C The material exhibited protonic, oxygen ionic and electronic conduction simultaneously in air, resulting in a good electrode performance. The performance of the BCSC cathode was similar with some reported composite cathode and can be improved with further microstructure optimization. The surface dissociative adsorption of O_2, electron charge transfer and diffusion of O^-_{ad} species were the rate determining steps for the electrode reaction. In addition, the BCSC cathode demonstrated good thermal expansion compatibility with the BCS electrolyte. These preliminary results demonstrate that $BaCe_{0.4}Sm_{0.2}Co_{0.4}O_{3-\delta}$ is a potential candidate cathode for SOFC-H.

References

[1] K.D. Kreuer, Annu. Rev. Mater. Res. 33 (2003) 333.
[2] L. Yang, S. Wang, K. Blinn, M. Liu, Z. Liu, Z. Cheng, M. Liu, Science 326 (2009) 126.
[3] E. Fabbri, D. Pergolesi, E. Traversa, Chem. Soc. Rev. 39 (2010) 4355.
[4] F. He, T. Wu, R. Peng, C. Xia, J. Power Sources 194 (2009) 263.
[5] T. Wu, Y. Zhao, R. Peng, C. Xia, Electrochim. Acta 54 (2009) 4888.
[6] E. Fabbri, S. Licoccia, E. Traversa, E.D. Wachsman, Fuel Cells 9 (2009) 128.
[7] V.B. Vert, C. Solís, J.M. Serra, Fuel Cells 11 (2011) 81.
[8] T. Shimura, H. Tanaka, H. Matsumoto, T. Yogo, Solid State Ionics 176 (2005) 2945.
[9] L. Yang, S. Wang, X. Lou, M. Liu, Inter. J. Hydrogen Energy 36 (2011) 2266.
[10] H. Matsumoto, T. Shimura, T. Higuchi, H. Tanaka, K. Katahira, T. Otake, K. Yashiro, A. Kaimai, T. Kawada, J. Mizusaki, J. Electrochem. Soc. 152 (2005) A488.
[11] C. Zhang, H. Zhao, S. Zhai, Inter. J. Hydrogen Energy 36 (2011) 3649.
[12] Y. Cheng, H. Zhao, D. Teng, F. Li, X. Lu, J. Membrane Sci. 322 (2008) 484.
[13] A. Nagy, G. Mestl, Appl. Catal. A: Gen. 188 (1999) 337.
[14] F.H. van Heuveln, H.J.M. Bouwmeester, J. Electrochem. Soc. 144 (1997) 134.